Jurnal Teknologi

Full Paper

SILVER NANOPARTICLES-AQUEOUS LEAF EXTRACT OF SIDAGURI *(Sida rhombifolia)* AS REDUCING AGENTS

Fatimah Fatimah[a,b], Abdul Wahid Wahab[b*], Abdul Karim[b], St. Fauziah[b], A. R. Pratiwi Hasanuddin[a], Arini Rajab[b,c], Muriyati Muriyati[d], Islawati[e], Subakir Salnus[b,f]

[a]Department of Medical Laboratory Technology, Stikes Panrita Husada, Bulukumba, 92561, Indonesia
[b]Department of Chemistry, Faculty of Mathematics and Natural Science, Hasanuddin University, Makassar, 90245, Indonesia
[c]Department of Environmental Management, Samarinda State Agricultural Polytechnic, Samarinda, 75242, Indonesia
[d]Department of Nursing, Stikes Panrita Husada, Bulukumba, 92561, Indonesia
[e]Department of Chemistry Education, State University of Makassar, Makassar,90222, Indonesia
[f]Department of Chemistry, State University of Makassar, Makassar, 90222, Indonesia

Article history
Received
5 April 2024
Received in revised form
10 July 2024
Accepted
23 July 2024
Published Online
22 December 2024

*Corresponding author
wahidwahab@unhas.ac.id

Graphical abstract

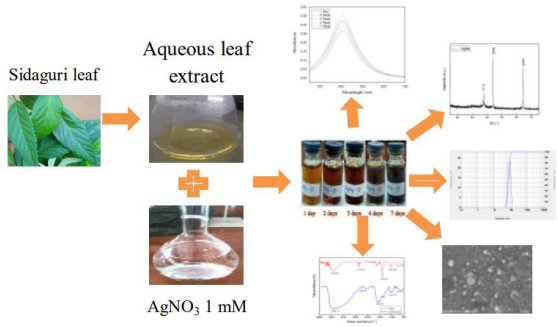

Abstract

The Sidaguri leaf, scientifically known as *Sida rhombifolia*, is a plant species rich in flavonoids that have the ability to act as reducing agent in formation of silver nanoparticles. This study presented the synthesis of silver nanoparticles (AgNp-Sid) using aqueous leaf extract of sidaguri. This study utilized a concentration ratio of 2:90 mL aqueous leaf extract of Sidaguri and $AgNO_3$ 1 mM. The size and morphology of AgNp-Sid was measured using UV-Visible Spectrophotometer, PSA, FT-IR, SEM-EDS, and XRD. The investigation revealed an ordinary particle size of 63.5 nm with polydispersity index (PI) of 0.284. The maximum wavelength varies between 405.4 nm and 407.8 nm with the increasing of time. AgNp-Sid exhibited a spherical morphology and had a crystalline structure that is face-centered cubic. The results suggested that the aqueous leaf extract of sidaguri had the ability to function as a reducing agent in the synthesis of silver nanoparticles, offering a safe, cost-effective, and environmentally friendly alternative.

Keywords: Aqueous leaf extract, Silver nanoparticles, *Sida rhombifolia*, reducing agent

© 2025 Penerbit UTM Press. All rights reserved

1.0 INTRODUCTION

Currently, nanotechnology is an important part of the development of modern research. Nanoparticles are part of nanotechnology, which is growing fast from year to year. Unlike massive substances, the characteristics of nanoparticles are based on size, shape, and surface morphology [1]. One type of metal that is widely studied as nanoparticles is metallic silver (Ag). Physical and chemical methods can be used to create silver nanoparticles. It is, however, very expensive and emits toxic substances into the environment. As a result, an alternative method for producing silver nanoparticles is required. Synthesis using biological materials, such as plant extracts, is a safe, biocompatible, and environmentally friendly option [2].

Silver nanoparticles derived from biological materials, particularly plant extracts, are also small and have a large surface area [3]. Silver nanoparticle synthesis using aqueous plant extracts has made significant progress because it is simpler, more cost-effective, and produces more stable materials [4]. This method does not involve elevated pressure, energy, temperature, or the addition of hazardous chemicals.

As a result, a growing number of researchers are currently utilizing biological techniques to synthesize silver nanoparticles by utilizing aqueous plant extracts as reducing agents. A wide range of botanical species have been employed as reducing agents in the synthesis of silver nanoparticles, including *Galega officinalis* [5], *Piper chaba* [6], *Pluchea indica L.* [7], *Psidium guajava Linn* [8], *Melia azedarach* [9], *Pandanus atrocarpus* [10], *Morinda citrifolia L.* [11], *Nymphae odorata* [12] and *Atropa acuminate* [13].

Biological methods using plant extracts as reducing agents can provide controlled particle size and shape [14]. Silver nanoparticles with plant extracts can be more stable and can minimize the risk of contamination with hazardous chemicals [15]. The manufacture of silver nanoparticles involves two primary steps. Firstly, Ag^0 is produced from reduction of Ag^+ ions that is carried out by the reducing agent. Secondly, the particle size is stabilised through a separate procedure [16].

One example is the Sidaguri (*Sida rhombifolia*) plant. Sidaguri plants' aerial parts contain several compounds such as quindolinone, 11-methoxy-quinoline, quindolin, cryptolepine, tetracontane, tetrapentacontane, scopoletin, scoparon, and ethoxy-ferulic, palmitic acid, linoleic acid, docosanoid acid, octodecanoid acid, elcosanoid acid, 5,7-dihydroxy-4'-Methoxyflavone (Acacetin) [17]. Active substances found in sidaguri plants allow for the formation of silver nanoparticles, which has reducing agent properties.

Hence, the ultimate goal of this investigation was to synthesize stable silver nanoparticles by a fast, simple, eco-friendly, and cost-effective using the aqueous leaf extract of sidaguri. The presence of silver ions in $AGNO_3$ solution, when exposed to sidaguri leaf extract, underwent reduction and led to a colour transformation to dark brown, indicating the creation of silver nanoparticles. The silver nanoparticles were synthesized and then characterized using UV-Visible Spectrophotometer, Particle Size Analyzer (PSA), Fourier Transform-Infrared Spectroscopy (FT-IR), X-ray diffraction (XRD), and Scanning Electron Microscopy-Energy Dispersive X-ray Spectroscopy (SEM-EDS) to confirming the formation of silver nanoparticles.

2.0 METHODOLOGY

2.1 The Preparation of the Aqueous Leaf Extract of Sidaguri

The plants used for this study were the fresh leaves (half part from the shoot) of Sidaguri collected from the Kera-Kera urban village in Makassar Regency, Indonesia. Before being used, sidaguri leaves were extensively cleaned with double-distilled water to dispose of any dirt and debris that had adhered to the leaves. After cleaning, the leaves were left to dry naturally at the ambient temperature of the room. These dried up leaves were then divided into tiny fragments. 5 g of cut dried leaves were put into a beaker glass and poured as much as 100 mL double-distilled water and subsequently scorching until boiling for 5 minutes [18]. Filtered paper (Whatmann No. 42) was used to filter the extract once it had cooled to ambient temperature. Extract is stored in refrigerator when not used.

2.2 Synthesis of AgNp-Sid

Silver nitrate ($AgNO_3$, 169, 87 g/mol) purchased from Merck and Whatman filtered paper no. 42 were used. All solutions were prepared with double-distilled water (Water One) for analytical laboratory use. $AgNO_3$ 1 mM solutions were prepared by disintegrating 0.085 g of $AgNO_3$ powder (Merck) in 500 mL in a volumetric flask with double-distilled water. $AgNO_3$ 1 mM solution is prepared and available for synthesizing of silver nanoparticles (AgNPs-Sid). AgNPs-Sid was produced by vigorously mixing 2 mL aqueous leaf extract of sidaguri with 90 mL of $AgNO_3$ 1 mM solution for two hours. A brownish color indicated the effective completion of the synthesis AgNPs-Sid. The pure AgNPs-Sid were acquired through freeze-dryer (Armfield) with temperature -53 °C and pressure 0.8 Mbar for further characterization.

2.3 Characterization of AgNp-Sid

2.3.1 UV-VIS Spectrophotometer

Characterization was performed on AgNPs-Sid using (Shimadzu 1800). The maximum wavelength of

colloidal AgNPs-Sid was determined in the wavelength range of 400-700 nm over the course of 1, 2, 3, 4 and 7 days.

2.3.2 Particle Size Analyzer (PSA)

The Particle Size Analyzer (SZ-100), from Horiba Scientific was utilized in order to ascertain the size distribution of AgNPs-Sid. Scattering angle of the measurement was 90° with temperature of the holder 25 °C.

2.3.3 Fourier Transform-Infrared Spectroscopy (FT-IR)

The infrared spectrum of the functional groups that may exist in AgNPs-Sid was analyzed with Fourier Transform-Infra Red Spectroscopy by IRPrestige-21 Shimadzu Corp. AgNPs-Sid was mixed with KBr crystals as a beam splitter. The measurement was in wavenumber range 500-4000 cm^{-1}.

2.3.4 X-Ray Diffraction (XRD)

The crystallite size of the AgNPs-Sid were determined by X-Ray Diffraction (XRD) analysis on a Shimadzu 7000 instrument, utilizing Cu Ka radiation (λ = 1.54 Å) and 2θ range of 20° to 70°. The Scherer equation can be utilized to calculate the mean crystal size as shown in equation (1) [18]:

$$D = \frac{k\,\lambda}{\beta \cos\theta} \quad (1)$$

The variables used in this context are λ for the wavelength of the X-ray source, D for the crystal size, k for the Scherrer constant, β for the full width half-maximum measured, and θ for Bragg's angle.

2.3.5 Scanning Electron Microscopy-Energy Dispersive X-ray Spectroscopy (SEM-EDS)

The surface morphology of the AgNPs-Sid were examined using Scanning Electron Microscopy (SEM) by Hitachi SU3500 with Accelerating Voltage 10 kV and Magnification 100x. The formation of AgNPs-Sid was also confirmed using Energy Dispersive X-ray Spectroscopy (EDS) by EDAX TEAM to determine the elemental composition.

3.0 RESULTS AND DISCUSSION

The AgNPs-Sid was effectively synthesized using leaf extract of sidaguri by adding silver nitrate solution. The color transitions from dark yellow shade to a dark brown hue during a timeframe of 1 to 7 days. Figure 1 displays the color changes during a 7-days period. The change in color of AgNPs-Sid indicates that surface plasmon oscillations have been stimulated [19]. The AgNPs-Sid synthesis process undergoes surface plasmon resonance, resulting in a color transition from dark yellow to brown, and further to dark brown. As time progresses, the color of AgNPs-Sid gradually intensifies into a darker shade of brown. An assessment of the stability of AgNPs-Sid was conducted by characterizing them using UV-Vis spectrophotometer. Figure 2 exhibits the UV-Vis absorption spectrum of AgNPs-Sid.

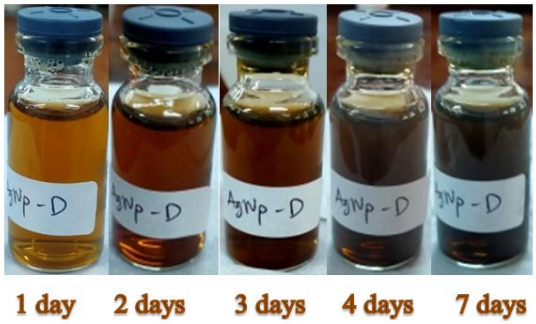

Figure 1 The changing color of AgNPs-Sid for 7 days

From the result can be suggested that the leaf extract of sidaguri contribute significantly in the formation of AgNPs-Sid. Based on Hawar, et. al., [20] there was an enormous compounds from the extract solution that have a role in the conversion of ion Ag^{+} into Ag^{0} in forming silver nanoparticles. Singla, et. al., [21] also confirmed that many compounds of leaf extract *that made* the changing colors of silver nanoparticles.

Analysis of UV-Vis Spectrophotometer was observed at the wavelength range of 250-700 Nm. The ultraviolet-visible (UV-Vis) absorption spectrum of AgNPs-Sid demonstrated a sharp peak from 405.4 Nm to 407.8 Nm. The peaks observed are likely attributed to the excited longitudinal surface plasmon vibrations of the silver nanoparticles, which may also be related to the nanospherical shape. These findings align with earlier data indicating that the wavelength of AgNPs-Sid falls within the 400–500 nm range [22]. Figure 2 showed that the absorbance increase over time.

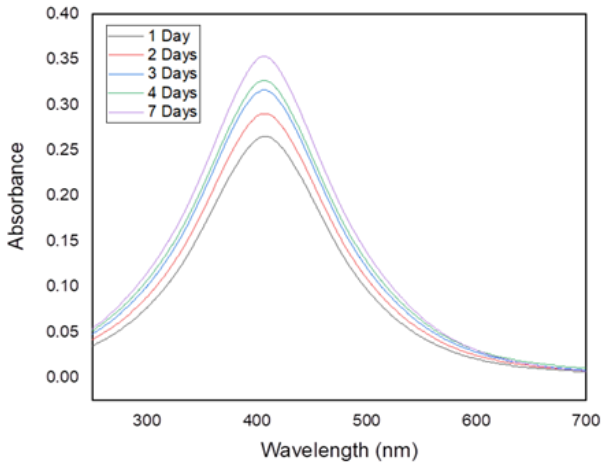

Figure 2 The UV-Visible absorbance spectrum ofAgNPs-Sid

Consistent with prior studies, the absorption peak's strength increased as time progressed [23]. The result also demonstrated a consistent peak throughout time, demonstrating the stability of the AgNPs-Sid [24]. Leaf extract of sidaguri can influence the increase in absorbance and stability that occurs in AgNP-Sid formation. The higher the amount of secondary metabolites contained in the extract, the more stable the size of the silver nanoparticles produced. [25]. On the first day of the AgNp-Sid synthesis process, only a small amount of Ag^{+} was reduced to Ag^{0}, and the following day, there was a significant increase in absorbance until Ag^{+} was completely reduced to Ag^{0}. The UV-Visible Surface Plasmon Resonance (SPR) is extremely responsive to the dimensions and morphology of the silver nanoparticles that are formed [21]. Single SPR band of AgNPs-Sid that reveals the spherical shape can be seen in Figure 2.The spherical shape from silver nanoparticles can be marked by a single SPR band range from 300-700 nm [26] [1].

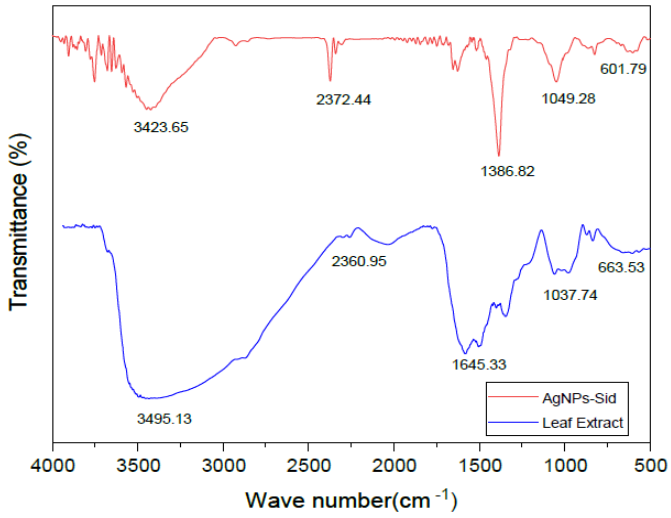

Figure 3 FTIR Spectrum of AgNPs-Sid

Figure 3 exhibits the Fourier Transform-Infrared (FT-IR) spectrum of AgNPs-Sid. The FTIR spectra were utilized in order to discern the functional groups enclosed within AgNPs-Sid. An absorption peak was detected at 500 to 4000 cm^{-1}. The FTIR spectrum, shown in Figure 3, displays a dominant absorption peak for the AgNPs-Sid at 3423.65, 2372.44, 1386.82, 1049.28, 601.79 cm^{-1}. The absorption peak ascribed from the stretching vibration of –OH functional groups (3423.79 cm^{-1}) in phenol, alcohols and flavonoids [27], the peak at 2372.44 cm^{-1} ascribed to O=C=O stretching owing to the flavonoid of the extract [21], 1386.82 as the bending vibration of the functional group of O-H [28], peak at 1049.28 cm^{-1} indicating C-O stretching [29] and peak at 601.79 cm^{-1} owing to C-Cl stretching the vibration of alkyl halides [30][31].

The FTIR spectrum of leaf extract of sidaguri showed an intense absorption peak at 3495.13, 2360.95, 1645.33, 1037.74, and 663.53 cm^{-1}. Based on the result, can be seen there were the shifted spectrum between the AgNPs-Sid and leaf extract of sidaguri. According to Singla, et. al., [21] the shifting peak in the spectrum suggests that the functional group in the leaf extract plays a crucial role in the binding process with silver nanoparticles. Silver nanoparticles can adsorb the functional groups content in plant extracts, which stabilizes them and prevents aggregation [31]. The changes in all the peaks show that leaf extracts of sidaguri functional groups can be used as reducing agents to make AgNPs-Sid.

Particle Size Analyzer (PSA) was utilized to ascertain the mean size of the AgNPs-Sid and the average size distribution. The characterization determined with scattering light intensity methods, 90° scattering angle and temperature 25°C. Figure 4 displays the mean size of AgNPs-Sid. This resulted Polydispersity distribution with an average size 63.5 nm and poly dispersity index (PI) 0.280. Based on Kasim, et. al., [32] polydispersity index value, the more it closer to zero (0) the more it getting better in distribution of sizes and physical stability.

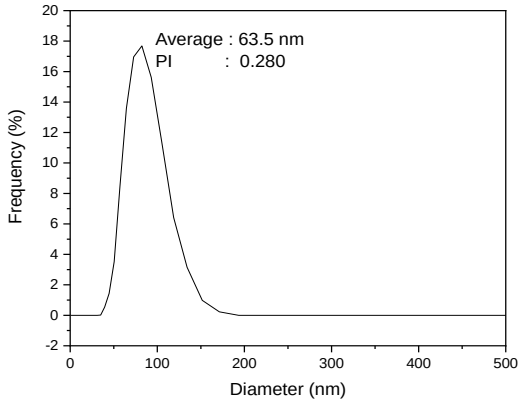

Figure 4 An average size of AgNPs-Sid

Figure 5 illustrates the mean size distribution of AgNPs-Sid. The range of principal particle sizes observed in AgNPs-Sid was calculated to be between 41-60 nm with percentage 8.46 %, 61-80 nm with percentage 16.96 %, 81-100 nm with percentage 15.62 %, 101-120 nm with percentage 6.42 %, 121-140 nm with percentage 3.15 %, 141-160 nm with percentage 0.98 %, and 161-180 nm with percentage 0.23 %.

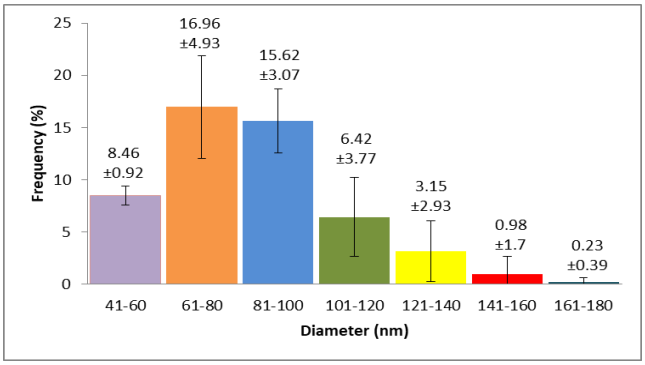

Figure 5 Representative average size distribution (n = 3) of AgNPs-Sid

Figure 6 displays XRD pattern of AgNPs-Sid. The technique of XRD is prior to ascertain the crystallite arrangement of silver nanoparticles. The XRD pattern has peaks at 37.79°, 44.047°, and 64.426°, which closely coincide to the lattice planes 111, 200, and 220, respectively. The XRD pattern was compared to the normal JCPDS card with the identification number 04-0783 [23]. The Scherer equation is employed for calculating the size of crystallites in AgNPs-Sid (Table 1).

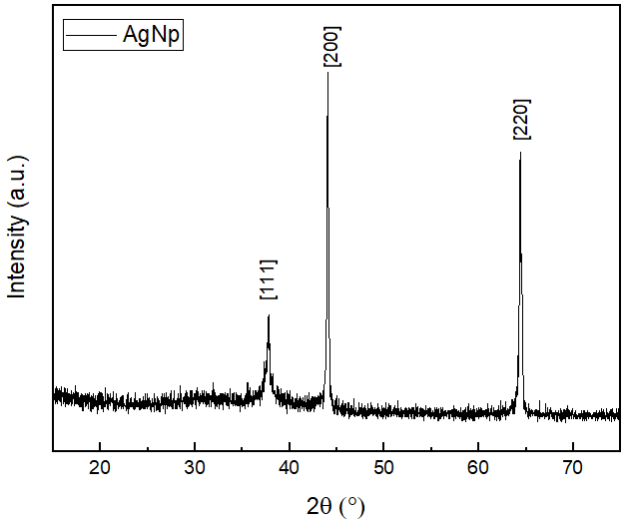

Figure 6 The XRD pattern of AgNPs-Sid

This research suggests that the crystallite Framework of AgNPs-Sid is face centered cubic. These outcomes were the consequence of the preceding discovery, which established the face-centered cubic structure of silver nanoparticles [29][30][33][34][35].

Table 1 Crystallite size determination of AgNPs-Sid

The Standard of 2θ peak JCPDS 04-0783	2θ peak of this study	*hkl*	FWHM	Crystallite size (Nm)
38.116	37.790	111	0.22970	39.80
44.277	44.047	200	0.17320	53.88
64.426	64.411	220	0.19370	52.78
		Average crystallite size:		48.82

Figure 7 displays the surface morphology of AgNPs-Sid. Figure 7 shows an image at a size of 10 µm with a magnification of 5000x and demonstrate nanoparticle aggregation affecting size variety. An analysis of the elemental composition and surface morphology of AgNPs-Sid Utilized SEM-EDS [36].

Kanimozhi, et. al., [37] hypothesized that the agglomeration could have occurred because of the extract's presence. Another work also disclosed the *Eichornia crassipes* [32], *Psidium guajava Linn*. [8], and *Zingiber officinale* [39].

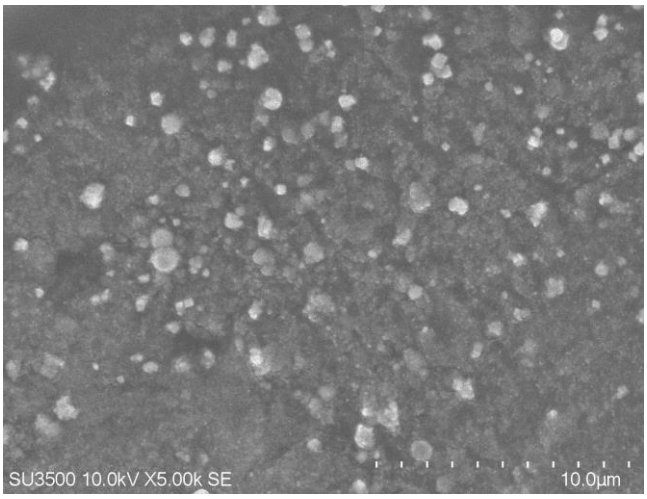

Figure 7 Characteristics of surface morphology of AgNPs-Sid

Figure 8 describes the elemental analysis of AgNPs-Sid. The signal of silver can be seen in 3 keV same as the previous report also showed the distinctive signal of silver at 3 keV [33][40]. This signal response was due to the characteristic of the metallic silver absorption [40]. As can be seen in Figure 8, metallic silver seem to be predominated among the element observed in the EDX spectrum. The proportion of metallic silver was considerably higher compared to other chemical elements, as silver (Ag) 74.05%, Oxygen (O) 25.14% and Chloride (Cl) 0.81%. The substantial proportion of metallic silver indicates that the leaf extract of sidaguri has the potential to contribute to the production of silver nanoparticles.

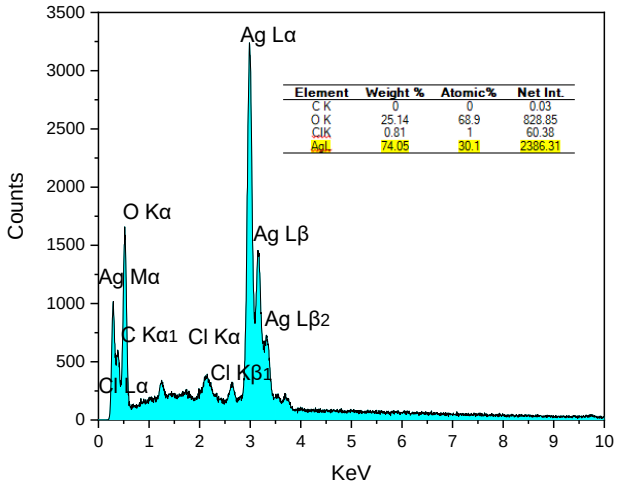

Figure 8 EDS Spectrum of AgNPs-Sid

4.0 CONCLUSION

On this worked, silver nanoparticles were successfully produced with biological method using the aqueous leaf extract of sidaguri. The characterization results demonstrate that aqueous leaf extract of sidaguri can function as a reducing agent for the production of silver nanoparticles, providing a safe, low cost and eco-friendly approach. The utilization of green plant resources as a reducing agent for the eco-friendly production of silver nanoparticles holds enormous potential for advancing biosensor applications. Green plant extracts containing silver nanoparticles can serve as substitutes for enzymes in the production of biosensors, resulting in cost and time savings while maintaining sensitivity and accuracy. In future endeavors, our focus will mostly be on the amalgamation of silver nanoparticles derived from aqueous extracts of green plants for implementation in biosensor applications.

Acknowledgement

We would like to extend our appreciation to the Center for Education Financial Services (BPPT Indonesia) and the Indonesia Endowment Funds for Education (LPDP Indonesia) for providing financial support for this research.

Conflicts of Interest

The author(s) declare(s) that there is no conflict of interest regarding the publication of this paper.

References

[1] S. Khalil *et al.* 2023. Antibacterial, Antioxidant and Photocatalytic Activity of Novel Rubus Ellipticus Leaf Mediated Silver Nanoparticles. *J. Saudi Chem. Soc.* 27(1): 101576. Doi: 10.1016/j.jscs.2022.101576.

[2] S. Jadoun, R. Arif, N. K. Jangid, and R. K. Meena. 2021. Green Synthesis of Nanoparticles using Plant Extracts: A Review. *Environ. Chem. Lett.* 19(1): 355–374. Doi: 10.1007/s10311-020-01074-x.

[3] C. Singh *et al.* 2019. Green Synthesis of Silver Nanoparticles using Aqueous Leaf Extract of Premna Integrifolia (L.) Rich in Polyphenols and Evaluation of Their Antioxidant, Antibacterial and Cytotoxic Activity. *Biotechnol. Biotechnol. Equip.* 33(1): 359–371. Doi: 10.1080/13102818.2019.1577699.

[4] S. Ahmad *et al.* 2019. Green Nanotechnology: A Review on Green Synthesis of Silver Nanoparticles — An Ecofriendly Approach. *Int. J. Nanomedicine*. 14: 5087–5107. Doi: 10.2147/IJN.S200254.

[5] F. Azimi, F. Mahmoudi, and M. M. Amini. 2021. Synthesis of Silver Nanoparticles by Galega Officinalis and Its Hypoglycemic Effects in Type 1 Diabetic Rats. *Nanomed. J*, 8(4): 255–263. Doi: 10.22038/NMJ.2021.59391.1613.

[6] M. Mahiuddin, P. Saha, and B. Ochiai. 2020. Green Synthesis and Catalytic Activity of Silver Nanoparticles based on Piper Chaba Stem Extracts. *Nanomaterials*. 10(9): 1–15. Doi: 10.3390/nano10091777.

[7] Fatimah, W. Wahab, and A. Karim. 2019. Synthesis of Silver Nanoparticles Using Beluntas Leaf (Pluchea Indica L.) Extract. *Indones. Chim. Acta*. 12(1): 7–12.

[8] V. Sandhiya, B. Gomathy, S. M. Rm, P. Thirunavukkarasu, M. R. A, and S. Asha. 2021. Green Synthesis of Silver Nanoparticles from Guava (Psidium guajava Linn.) Leaf for Antibacterial, Antioxidant and Cytotoxic Activity on HT-29 Cells (Colon cancer). *Ann. R.S.C.B.* 25(6): 20148–20163.

[9] S. Jebril, R. Khanfir Ben Jenana, and C. Dridi. 2020. Green Synthesis of Silver Nanoparticles using Melia Azedarach Leaf Extract and Their Antifungal Activities: In Vitro and in Vivo. *Mater. Chem. Phys.* 248(March). Doi: 10.1016/j.matchemphys.2020.122898.

[10] A. H. Jabbar *et al.* 2020. Green Synthesis and Characterization of Silver Nanoparticle (AgNPs) using Green Synthesis and Characterization of Silver Nanoparticle (AgNPs) using Pandanus Atrocarpus Extract. *International Journal of Advanced Science and Technology*. 29(03): 4913–4922

[11] V. Morales-Lozoya *et al.* 2020. Study of the Effect of the Different Parts of Morinda citrifolia L. (noni) on the Green Synthesis of Silver Nanoparticles and Their Antibacterial Activity. *Appl. Surf. Sci.* 537(September): 147855. Doi: 10.1016/j.apsusc.2020.147855.

[12] A. Gudimalla, J. Jose, R. J. Varghese, and S. Thomas. 2021. Green Synthesis of Silver Nanoparticles Using Nymphae odorata Extract Incorporated Films and Antimicrobial Activity. *J. Polym. Environ.* 29(5): 1412–1423. Doi: 10.1007/s10924-020-01959-6.

[13] S. Rajput, D. Kumar, and V. Agrawal. 2020. Green Synthesis of Silver Nanoparticles using Indian Belladonna Extract and Their Potential Antioxidant, Anti-Inflammatory, Anticancer and Larvicidal Activities. *Plant Cell Rep.* 39(7): 921–939. Doi: 10.1007/s00299-020-02539-7.

[14] H. B. Habeeb Rahuman *et al.* 2022. Medicinal plants Mediated the Green Synthesis of Silver Nanoparticles and Their Biomedical Applications. *IET Nanobiotechnology*. 16(4): 115–144. Doi: 10.1049/nbt2.12078.

[15] C. P. Devatha and A. K. Thalla. 2018. *Green Synthesis of Nanomaterials*. Elsevier Ltd.

[16] A. B. Junaidi and A. Wahyudi. 2015. Kajian Sintesis Nanopartikel Perak Pada Komposit Kitosan Dan Polietilena Glikol: Efek Jenis Agen Pereduksi Organik. *Proceeding Chemistry National Seminar*. 148–156.

[17] O. S. Chaves *et al.* 2013. Secondary Metabolites from Sida rhombifolia L. (Malvaceae) and the Vasorelaxant Activity of Cryptolepinone. *Molecules*. 18(3): 2769–2777. Doi: 10.3390/molecules18032769.

[18] H. Heryanto *et al.* 2022. Favourable Peak Diffraction Shift Moments as a Function of Mg Doping on ZnO Matrix as a Promising Catalyst for Methylene Blue w"ecorum Leaf Extract and Evaluation of Their Cytotoxicity and Antifungal Activity. *J. Nanomater.* 2022. Doi: 10.1155/2022/1058119.

[21] S. Singla, A. Jana, R. Thakur, C. Kumari, S. Goyal, and J. Pradhan. 2022. Green Synthesis of Silver Nanoparticles using Oxalis Griffithii Extract and Assessing Their Antimicrobial Activity. *OpenNano*. 7(April): 100047. Doi: 10.1016/j.onano.2022.100047.

[22] N. S. Alharbi, N. S. Alsubhi, and A. I. Felimban. 2022. Green Synthesis of Silver Nanoparticles using Medicinal Plants: Characterization and Application. *J. Radiat. Res. Appl. Sci.* 15(3): 109–124. Doi: 10.1016/j.jrras.2022.06.012.

[23] S. Dangi, A. Gupta, D. K. Gupta, S. Singh, and N. Parajuli. 2020. Green Synthesis of Silver Nanoparticles using Aqueous Root Extract of Berberis Asiatica and Evaluation of Their Antibacterial Activity. *Chem. Data Collect.* 28. Doi: 10.1016/j.cdc.2020.100411.

[24] M. Hekmati, S. Hasanirad, A. Khaledi, and D. Esmaeili. 2020. Green Synthesis of Silver Nanoparticles using Extracts of Allium Rotundum L, Falcaria Vulgaris Bernh, and Ferulago Angulate Boiss, and Their Antimicrobial Effects in Vitro. *Gene Reports*. 19(October 2019). Doi: 10.1016/j.genrep.2020.100589.

[25] I. N. Oktavia and S. Sutoyo. 2021. Article Review: Synthesis

of Silver Nanoparticles using Bioreductor from Plant Extract as an Antioxidant. *Unesa J. Chem.* 10(1): 37–54.

[26] H. Yousaf, A. Mehmood, K. Shafique, and M. Raffi. 2020. Materials Science & Engineering C Green Synthesis of Silver Nanoparticles and Their Applications as an Alternative Antibacterial and Antioxidant Agents. *Mater. Sci. Eng. C*. 112(October 2019): 110901. Doi: 10.1016/j.msec.2020.110901.

[27] M. Sharifi-Rad, H. S. Elshafie, and P. Pohl. 2024. Green Synthesis of Silver Nanoparticles (Agnps) by Lallemantia Royleana Leaf Extract: Their Bio-Pharmaceutical and Catalytic Properties. *J. Photochem. Photobiol. A Chem.* 448(September 2023): 115318. Doi: 10.1016/j.jphotochem.2023.115318.

[28] E. N. Gecer, R. Erenler, C. Temiz, N. Genc, and I. Yildiz. 2022. Green Synthesis of Silver Nanoparticles from Echinacea Purpurea (L.) Moench with Antioxidant Profile. *Part. Sci. Technol.* 40(1): 50–57. Doi: 10.1080/02726351.2021.1904309.

[29] M. T. Yassin, F. O. Al-Otibi, A. A. F. Mostafa, and A. A. Al-Askar. 2022. Facile Green Synthesis of Silver Nanoparticles Using Aqueous Leaf Extract of Origanum majorana with Potential Bioactivity against Multidrug Resistant Bacterial Strains. *Crystals*. 12(5). Doi: 10.3390/cryst12050603.

[30] A. Sharma, A. Sagar, J. Rana, and R. Rani. 2022. Green Synthesis of Silver Nanoparticles and Its Antibacterial Activity using Fungus Talaromyces Purpureogenus Isolated from Taxus baccata Linn. *Micro Nano Syst. Lett.* 10(2): 1–12. Doi: 10.1186/s40486-022-00144-9.

[31] A. W. Alshameri, M. Owais, I. Altaf, and S. Farheen. 2022. Rumex Nervosus Mediated Green Synthesis of Silver Nanoparticles and Evaluation of Its In Vitro Antibacterial, and Cytotoxic Activity. *OpenNano*. 8(July): 100084. Doi: 10.1016/j.onano.2022.100084.

[32] S. Kasim, P. Taba, F. Matematika, P. Alam, and U. Hasanuddin. 2020. Sintesis Nanopartikel Perak Menggunakan Ekstrak Daun Eceng Gondok (Eichornia crassipes) Sebagai Bioreduktor. *Kovalen J. Ris. Kim.* 6(2): 126–133.

[33] A. Naseer, M. Iqbal, S. Ali, A. Nazir, M. Abbas, and N. Ahmad. 2022. Green Synthesis of Silver Nanoparticles using Allium Cepa Extract and Their Antimicrobial Activity Evaluation. *Chem. Int.* 8(3): 89–94.

[34] M. A. Al Mashud *et al.* 2022. Green Synthesis of Silver Nanoparticles using Cinnamomum tamala (Tejpata) Leaf and their Potential Application to Control Multidrug Resistant Pseudomonas Aeruginosa Isolated from Hospital Drainage Water. *Heliyon*. 8(7): e09920. Doi: 10.1016/j.heliyon.2022.e09920.

[35] H. Basalius *et al.* 2023. Green Synthesis of Nano-silver using Syzygium Samarangense Flower Extract for Multifaceted Applications in Biomedical and Photocatalytic Degradation of Methylene Blue. *Appl. Nanosci.* 13(6): 3735–3747. Doi: 10.1007/s13204-022-02523-5.

[36] M. Oves *et al.* 2022. Green Synthesis of Silver Nanoparticles by Conocarpus Lancifolius Plant Extract and Their Antimicrobial and Anticancer Activities. *Saudi J. Biol. Sci.* 29(1): 460–471. Doi: 10.1016/j.sjbs.2021.09.007.

[37] S. Kanimozhi *et al.* 2022. Biogenic Synthesis of Silver Nanoparticle using Cissus Quadrangularis Extract and Its Invitro Study. *J. King Saud Univ. - Sci.* 34(4): 101930. Doi: 10.1016/j.jksus.2022.101930.

[38] F. Chen, Q. Zheng, X. Li, and J. Xiong. 2022. Citrus Sinensis Leaf Aqueous Extract Green-synthesized Silver Nanoparticles: Characterization and Cytotoxicity, Antioxidant, and Anti-human Lung Carcinoma Effects. *Arab. J. Chem.* 15(6): 103845. Doi: 10.1016/j.arabjc.2022.103845.

[39] Y. Wang, A. Chinnathambi, O. Nasif, and S. A. Alharbi. 2021. Green Synthesis and Chemical Characterization of a Novel Anti-human Pancreatic Cancer Supplement by Silver Nanoparticles Containing Zingiber Officinale Leaf Aqueous Extract. *Arab. J. Chem*. 14(4): 103081. Doi: 10.1016/j.arabjc.2021.103081.

[40] F. E. Ettadili *et al.* 2022. Green Synthesis of Silver Nanoparticles using Phoenix Dactylifera Seed Extract and Their Electrochemical Activity in Ornidazole Reduction. *Food Chem. Adv*. 2(July): 100146. Doi: 10.1016/j.focha.2022.100146.